Journal of Chromatography A, 1578 (2018) 28–34

Contents lists available at ScienceDirect

Journal of Chromatography A

journal homepage: www.elsevier.com/locate/chroma

Gradient elution behavior of proteins in hydrophobic interaction chromatography with a U-shaped retention factor curve under overloaded conditions

Arch Creasy[a,1], Joseph Lomino[b], Giorgio Carta[a,*]

[a] Department of Chemical Engineering, University of Virginia, Charlottesville, VA, USA
[b] Biologics Process Development, Bristol-Myers Squibb, Hopewell, NJ, USA

ARTICLE INFO

Article history:
Received 29 June 2018
Received in revised form 2 October 2018
Accepted 5 October 2018
Available online 7 October 2018

Keywords:
Hydrophobic interaction chromatography
Gradient elution
Proteins
Antibodies
U-shaped retention factor curves
Overloaded conditions

ABSTRACT

The gradient elution hydrophobic interaction chromatography of a monoclonal antibody that exhibits U-shaped retention as a function of the ammonium sulfate concentration is investigated for overloaded conditions at protein loads up to 30% of the column equilibrium binding capacity. Protein load and gradient slope affect both elution peak shape and protein recovery during the gradient. Higher protein loads result in tailing peaks with near 100% recovery that transition to fronting peaks and incomplete recovery as the protein load is reduced. The gradient slope also affects peak shape and recovery. Tailing peaks with lower recovery are obtained with sharper gradients and the most tailing peak and lowest recovery are obtained when step elution rather than gradient is implemented. Modeling the chromatographic elution based on independently determined adsorption isotherms as a function of protein and ammonium sulfate concentration predicts results in agreement with the experimental trends confirming that the unusual chromatographic behavior observed is due to the U-shaped protein binding as a function of the ammonium sulfate concentration. Although less pronounced than in the dilute limit, the U-shaped binding still produces peak shapes and recovery losses as a function of gradient slope that differ from those seen for systems where retention is a monotonic function of salt concentration.

1. Introduction

Hydrophobic interaction chromatography (HIC) is widely used for protein separations both in the laboratory and for manufacturing [1–3]. In this process, a kosmotropic salt, such as ammonium sulfate, drives reversible partitioning of proteins and other biopolymers between the mobile phase and the stationary phase surface. Normally, protein retention exhibits a monotonic dependence on the kosmotropic salt concentration with high concentrations facilitating partitioning toward the stationary phase and low concentrations facilitating HIC partitioning toward the mobile phase [4–6]. This trend mirrors, in an inverse way, the well-known effect of kosmotropes on protein solubility in aqueous solutions [7].

As shown by Melander and Horvath [4] and by Melander et al. [5], the solvophobic theory provides a basis for describing HIC by considering the Gibbs free energy differences between mobile and stationary phases that are associated with cavity formation, electrostatic effects, and van der Waals interactions. Accordingly, the protein retention factor in the linear region of the binding isotherm, k', is expressed as a function of the kosmotropic salt concentration, C_M, by [4,5]:

$$ln\left(k' - k'_M\right) = lnk'_0 - \frac{b\sqrt{C_M}}{1 + c\sqrt{C_M}} + \lambda C_M \quad (1)$$

where $k' = \phi\left(\varepsilon_p + K\right)$, $\phi = (1-\varepsilon)/\varepsilon$ is the phase ratio, ε is the extraparticle or external porosity, ε_p is the intraparticle or internal porosity, K is the protein Henry's constant describing protein binding, k'_M is the retention factor of the salt, and k'_0 is the protein retention factor at $C_M = 0$. If the salt is not bound, then $k'_M = \phi\varepsilon_p$. Although theoretically related to thermodynamic functions [5], in practice, the parameters k'_0, b, c and λ are usually treated as empirical constants determined by data fitting. It should be noted that although IUPAC [8] recommends the symbol k for the retention factor, for consistency with our previous paper [9] and with the earlier literature, we continue to use the symbol k' in this work.

* Corresponding author.
E-mail address: gc@virginia.edu (G. Carta).
[1] Current address: Pfizer, Andover, MA, USA.

https://doi.org/10.1016/j.chroma.2018.10.003
0021-9673/

At high values of C_M, the last term on the right hand side of Eq. (1) becomes dominant and this equation reduces to:

$$ln\left(k' - k'_M\right) = lnk'_0 - \frac{b}{c} + \lambda C_M = A + \lambda C_M \quad (2)$$

which gives the monotonic exponential dependence of retention on salt concentration normally observed for proteins in HIC. Because of this trend normally observed at high kosmostrope concentrations, HIC is most often operated with a gradient starting at high salt, where protein binding is promoted and ending at low salt or, often, with no salt [5,10]. Gradient operation generally improves robustness and is thought to prevent irreversible binding and/or denaturation [5]. Step elution with an abrupt change from high salt to no salt is also used for easier separations.

However, at low C_M values, the third term in Eq. (1) can become less important and k' values that decrease as C_M increases can be observed resulting in a U-shaped retention factor curve with a minimum k' that depends on the specific values of lnk'_0, b, c, and λ. Such a theoretical trend has in fact been observed by a number of authors including Melander et al. [5] for several proteins on a propyl-functionalized resin using $NaClO_4$, by Machold et al. [11] for lysozyme on a number of HIC resins using ammonium sulfate, and, more recently, by Creasy et al. [9] for both lysozyme and for a monoclonal antibody on the HIC resin Capto Phenyl (High Sub) also using ammonium sulfate. Several other cases where U-shaped retention factor curves have been observed are discussed in ref. [9].

In our prior work [9], we have developed a model based on the solvophobic theory expression of the retention factor to help understand the implications of a U-shaped retention factor curve on the behavior of gradient elution in HIC. For these conditions, we have shown that, with a steep gradient, low salt concentrations fed later in the gradient can overtake the protein that is moving down the column, causing it to rebind resulting, in turn, in reduced protein recovery. The normalized gradient slope, defined as the difference between initial and final salt concentration divided by the duration of the gradient in units of column volumes, was shown to determine whether the protein elutes in the gradient, partially elutes, or is virtually trapped in the column defining a critical gradient slope beyond where 100% recovery is no longer possible.

Although our prior work could explain and predict the effects of a U-shaped retention factor curve, the data and analysis were limited to the Henry's law region of the adsorption isotherm, which is observed at low loadings. In practice, of course, there is both practical and theoretical interest in understanding the behavior for overloaded conditions where protein binding becomes a non-linear function of protein concentration in the mobile phase, which is the scope of this work.

Adsorption isotherms at high protein loads are expected to be more complicated because, in addition to solvophobic effects, protein-protein interactions and surface saturation also affect binding [12]. Protein adsorption isotherms have been measured experimentally for different HIC adsorbents by several authors including, for example, Xia et al. [13], Chen and Cramer [14], Meng et al. [15], and Wang et al. [16]. The isotherms obtained by these authors were roughly Langmuirian in shape with binding strength always decreasing as the salt concentration decreased. The quantitative description of these isotherms is not straightforward, however. Mollerup [12] suggested a thermodynamic framework based on a stoichiometric binding model. Deitcher et al. [17] and Wang et al. [16] also used a stoichiometric model to describe HIC isotherms but their model took into account explicitly a release of water molecules at the protein–surface contact area. In both cases, exponential expressions for water activity coefficients were used to describe the effect of salt concentration on the isotherm. Xia et al. [13] used a preferential interaction model in conjunction with a polynomial (quadratic) Langmuir model, derived from statistical thermodynamics [18], which was able to describe HIC adsorption showing a monotonic effect of kosmotropic salt concentration both in the linear and in the non-linear regions of the isotherm.

The goal of this work is to extend our previous HIC studies of a protein exhibiting a U-shaped retention factor curve in HIC to the case of high protein loadings. Two important effects can be anticipated at higher loads. The first is that the isotherm will become non-linear affecting, in turn, the shape of the ensuing chromatograms. The second is that for highly overloaded gradient elution conditions, the protein will elute earlier in the gradient compared to the low loading case. Both effects are well understood for cases where retention increases monotonically with salt concentration but what happens when retention exhibits a minimum at intermediate salt is not exactly known. For this study, using the same antibody and resin of Creasy et al. [9], we measure adsorption isotherms over a range of protein and ammonium sulfate concentrations and perform overloaded linear gradient elution experiments varying both protein load and gradient slope. An empirical model is developed to describe the isotherm data and used to generate model predictions of column behavior based on an empirical interpolation method to describe the effect of salt concentrations.

2. Experimental

2.1. Materials

The resin used in this work is Capto Phenyl (High Sub) (GE Healthcare, Uppsala, Sweden). Basic properties of the resin (volume-average particle diameter d_p = 78 μm, intraparticle porosity ε_p = 0.91, and mean pore radius r_{pore} = 30 nm) were obtained in our prior work [9].

The protein used in this work is a monoclonal antibody (mAb) with pI∼8 and MW∼150 kDa, which was identified as "mAbB" in our prior work [9]. Chemicals used in buffer preparation (trisodium phosphate, phosphoric acid, and ammonium sulfate) were obtained from MilliporeSigma (St. Louis, MO, USA) and Fisher Scientific (Fair Lawn, NJ, USA).

2.2. Methods

The buffers used in this work were prepared by mixing trisodium phosphate and ammonium sulfate with distilled-deionized water to yield 30 mM Na^+ and the desired ammonium sulfate molarity. The pH was then adjusted to 7.2 by mixing in dropwise concentrated phosphoric acid. mAb solutions in the desired buffer were prepared by size exclusion chromatography with a HiPrep 26/10 desalting column from GE Healthcare (Piscataway, NJ, USA).

Adsorption isotherms at varying protein and ammonium sulfate concentrations were obtained by first equilibrating the resin in the desired buffer and then removing the extraparticle liquid by centrifugal filtration using 2 mL Corning Costar Spin-X microfiltration tubes (Sigma-Aldrich, St. Louis, MO, USA) with an Eppendorf Minispin bench-top centrifuge (Eppendorf North America, Hauppauge, NY, USA) for 15 min at 5000 rpm. Weighed samples of the filtered resin (15–300 mg) were then added to 2 mL plastic tubes and mixed with 1 mL of protein solution by slowly rotating the tubes end-over-end on a wheel for 24 h. After this time, supernatant samples were taken to determine the residual protein concentration using a NanoDrop 2000c UV–vis spectrophotometer (Thermo Scientific, Wilmington, DE, USA) at 280 nm. The total amount of protein held by the resin was then calculated by mass balance. Finally, the total protein concentration in the resin, $\bar{q}_p$, including both bound protein and protein just held in the particle pores, was calculated by divid-

ing this total amount by the volume of resin beads. The latter was determined by converting the mass of hydrated resin beads using their density of 1.04 g/mL, determined from pycnometer measurements.

Linear gradient elution (LGE) experiments were done with a 0.5 diameter × 20 cm long Tricorn column from GE Healthcare packed to a height of 18.8 cm with the Capto Phenyl resin as described in Creasy et al. [9]. The packing quality was determined by making pulse injections of NaCl in the 0.2 M ammonium sulfate buffer and recording the ensuing conductivity trace at the column outlet. The reduced HETP (defined as the HETP divided by the resin particle diameter) was 2.0 and the asymmetry factor was $A_s = 1.2$, indicating that the column was well packed. Gradient durations were defined in terms of CV units as the volume of mobile phase passed through the column divided by the column volume. The extraparticle or external porosity of this column was determined to be $\varepsilon = 0.41$ based on the retention of 2000 kDa dextran. Protein sample volumes between 1.1 and 5 mL containing approximately 1–4 mg/mL protein in 0.2 M ammonium sulfate were loaded using a 50 mL "Superloop" corresponding to protein loads ranging between 0.3–5.3 mg/mL of column. The column was first equilibrated with 0.2 M ammonium sulfate and eluted after loading either with a linear gradient to 0 M ammonium sulfate followed by a hold step for 5 CV at 0 M ammonium sulfate or with a step change to 0 mM ammonium sulfate followed by a hold step for 25 CV also at 0 M ammonium sulfate. After each elution, the column was stripped with 2 CV of 70% isopropyl alcohol in water and cleaned with 100 mM NaOH. Re-equilibration with the 0.2 M load buffer following strip and cleaning was fast requiring only about 2 CV. Starting with virgin resin, the column could be used repeatedly for at least 8 runs at various protein loads without affecting the retention time more than about 10%. Increasing the number of runs further resulted, however, in fouling of the column, requiring repacking with virgin resin in order to obtain consistent results.

All LGE experiments were performed using an AKTA Pure 25 system from GE Healthcare at a flow rate of 0.5 mL/min corresponding to a superficial velocity of 153 cm/h. UV280 and conductivity were recorded and converted to the corresponding protein and ammonium sulfate concentrations using independently obtained calibration curves. Appropriate time shifts of UV and conductivity signals were made to take into account the dead volumes between the column and the respective detectors. All experiments were conducted at room temperature, 21 ± 2 °C.

3. Results

3.1. Adsorption isotherms

Fig. 1 shows the isotherm data obtained at 0.2, 0.15, 0.1, 0.05, 0.025, and 0 M ammonium sulfate and protein concentrations spanning a range from about 0.1 to about 4 mg/mL. As seen in Fig. 1A, starting at 0.2 M ammonium sulfate, binding initially decreases as the salt concentration decreases down to 0.05 M but then increases again as the salt concentration is decreased further. At 0.025 M ammonium sulfate, the isotherm becomes almost indistinguishable from that obtained at 0.15 M. This behavior is consistent with the U-shaped retention factor curve obtained from isocratic elution experiments at low protein loads in our prior work [9], which exhibited a retention minimum at about 0.05 M ammonium sulfate. As seen from the present data, while the initial slope of the isotherm is consistent with the dilute k' trends, the shape of the isotherm also varies with salt concentration suggesting a complex interplay of salt and protein concentration effects on binding. As noted by Meng et al. [15], such shifts in isotherm shape may suggest a varying binding mechanism.

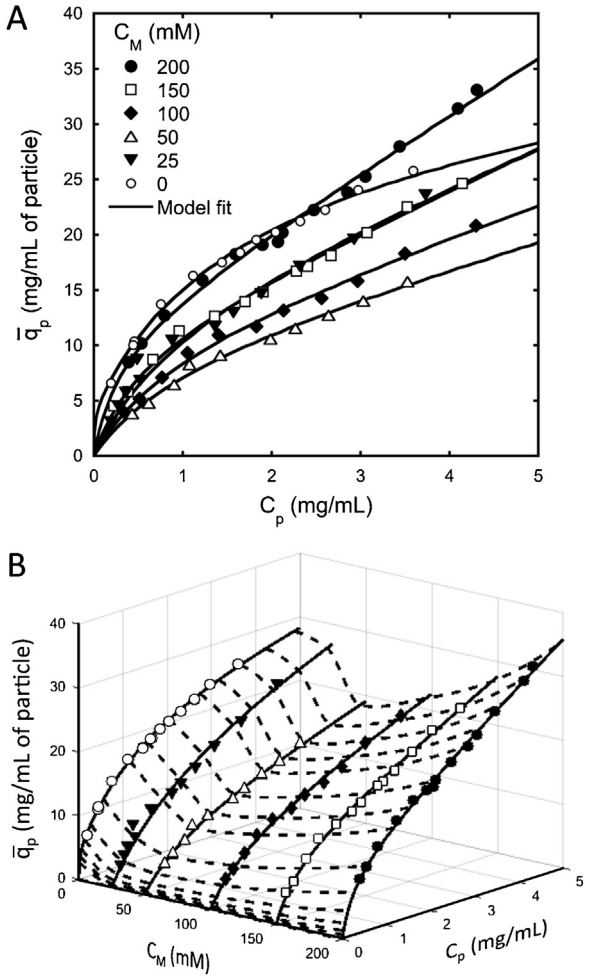

Fig. 1. Adsorption isotherm data at different ammonium sulfate concentrations C_M. Panel A shows the 2-dimensional view of the isotherms and panel B shows the 3-dimensional view with C_M as a third axis. Symbol legend in B is the same as in A. The solid lines are calculated with the quadratic Langmuir model with the parameters given in Table 1 fitted individually at each ammonium sulfate concentration C_M. The dashed lines are the PCHIP curves used to interpolate the effect of C_M.

3.2. Description of adsorption isotherms

None of the typical mechanistic models discussed in the Introduction were able to represent the complex binding behavior observed in this work. Thus, following Xia et al. [13] we used the quadratic Langmuir isotherm as an empirical function to fit the data at each salt concentration according to the following equation:

$$\bar{q}_p = \varepsilon_p C_p + \frac{K_e\left(a_1 C_p + a_2 C_p^2\right)}{1 + K_e\left(a_3 C_p + a_4 C_p^2\right)} \tag{3}$$

where the first term on the right hand side accounts for the protein held in the intraparticle porosity and the second terms accounts for the protein actually bound to the chromatographic surface. In this equation, $\bar{q}_p$ is the total protein concentration in the resin (including both the protein held in the pores and that bound to the hydrophobic surface), C_p is the protein concentration in solution, and K_e, a_1, a_2, a_3, and a_4 are salt-dependent constants that are determined independently at each salt concentration. This equation has sufficient flexibility to describe the effect of C_p at high protein concentrations and reduces to the linear relationship $\bar{q}_p = \left(\varepsilon_p + K_e a_1\right) C_p$ at low protein concentrations. In order to maintain consistency with the behavior measured previously in the dilute limit, K_e was related to the retention factor k' by the equa-

Table 1
Quadratic Langmuir isotherm parameters fitted to isotherm data independently at each ammonium sulfate concentration value, C_M. $K_e = (k' - k'_M)/\phi a_1$ where k' is calculated from Eq. (1) with lnk'_0 = 6.17, b = 45.7, c = 5.74, and λ = 17.9 with C_M in units of mol/L according to Ref. [9] to match the retention results at infinite dilution.

C_M (M)	K_e	a_1	a_2 (mL/mg)	a_3	a_4 (mL/mg)	Mean relative absolute deviation (%)
0.20	76.2	0.551	0.185	0.044	0	2.3
0.15	27.1	0.806	0.170	0.064	0	3.1
0.10	9.49	1.343	0.178	0.103	0	3.4
0.050	6.99	1.439	0.142	0.120	0	3.9
0.025	2.41	5.302	0.230	0.207	0	9.8
0	1025.0	0.352	1.518	0.081	0.051	2.0

tion $K_e = (k' - k'_M)/\phi a_1$ where k' is calculated from Eq. (1) using our previously determined parameter values [9]. The remaining parameters a_1, a_2, a_3, and a_4 were then determined by regressing the isotherm data at each salt concentration resulting in $6 \times 4 = 24$ model parameters associated with Eq. (3) to describe $\bar{q}_p$ as a function of C_p at each constant ammonium sulfate concentration. Thus, in this approach we have combined Eq. (1) (i.e. the solvophobic model) with the empirical Eq. (3) from Xia et al. to arrive at an overall description of the isotherms that, on one hand merges with the solvophobic model in the dilute limit, while, on the other it correctly predicts the isotherm shape at high protein loads. Table 1 provides a summary of these values along with the mean absolute deviation between data and regressed model at each salt concentration. Calculated lines are given in Fig. 1. The agreement between data and calculated values was within about ±4%, well within the experimental error of the isotherm data.

Because a mechanistic relationship between these parameter values and salt concentration was not found (except for K_e, which is described by Eq. (1)), the method of Creasy et al. [19,20] was used to correlate this effect using piecewise cubic Hermite interpolating polynomials (PCHIP) with MATLAB's 1D interpolating *pchip* function and predict isotherm values at intermediate values of C_M.

Fig. 1B shows a 3-D representation of the isotherm data, exhibiting an obvious cleft with minimum binding around 0.05 M ammonium sulfate, along with the fitted lines (solid) according to Eq. (3). The dashed lines in this figure show the curves generated by *pchip*. These lines run perpendicular to the fitted quadratic Langmuir curves and describe the effect of the ammonium sulfate concentration at constant values of the protein concentration C_p.

3.3. Gradient elution results

Figs. 2 and 3 show the experimental elution curves (dashed lines) as a function of protein load in the range 0.3–5.3 mg/mL with a 10 CV gradient and as a function of gradient length between 0 and 20 CV with a 5.3 mg/mL protein load, respectively. Since the equilibrium binding capacity of the mAb in the load buffer (0.2 M ammonium sulfate) is approximately 30 mg/mL and the extraparticle porosity is 0.41, the equilibrium binding capacity is about 18 mg/mL of column. Thus, these protein loads are between 1.6% and 30% of the column equilibrium binding capacity. Note, however, that the different loads were obtained through different combinations of load concentration and load volume (see the figure caption for detailed conditions). The corresponding protein recoveries calculated after 5 CV following the end of the gradient for the gradient runs and after 25 CV for the step elution case are shown in Fig. 4A and B for the runs at constant gradient slope and for those varying the gradient slope, respectively. As seen in Fig. 2, as the protein load increases, the peaks elute earlier along the gradient and at higher salt concentrations compared to the low-loading case. The peak shape also changes exhibiting pronounced tailing at the highest protein loads and pronounced fronting at the lowest load. Finally, as seen in Fig. 4A, protein recovery is also affected, increasing as the protein load increases. These trends are explained by the U-shaped adsorption behavior as a function of salt concentration. At the highest loads, elution occurs earlier because a substantial portion of the column is saturated with the feed. As a result, most of the protein has a chance to elute before being caught up by the low salt concentrations that would otherwise cause it to rebind. As a consequence, a high percentage recovery is obtained within the gradient. This is not the case at the lower protein loads where the protein elutes only late in the gradient so that a substantial fraction of the protein is rebound to the resin before being able to leave the column. As seen in Fig. 4A, with a 0.3 mg/mL load, even after 5 CV following the end of the gradient, recovery was only about 70%. Much longer volumes would be required to elute the remaining protein since retention becomes strong again at low salt.

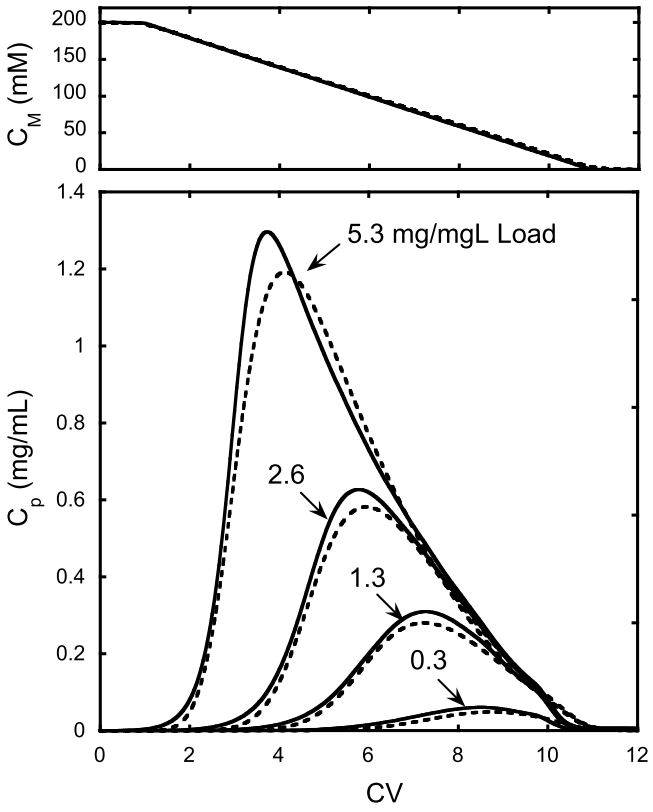

Fig. 2. Comparison of experimental gradient elution profiles (dashed lines) obtained at different protein loads as shown by curve labels with model predictions (solid lines) using a linear gradient from 0.2 to 0 M ammonium sulfate in 10 CV. Experimental loads were realized as follows: 0.97 mg/mL feed concentration with 1.1 feed volume (0.3 mg/mL load); 0.97 mg/mL feed concentration with 5 mL feed volume for 1.3 mg/mL load; 1.95 mg/mL feed concentration with 5 mL feed volume for 2.6 mg/mL load; 3.9 mg/mL feed concentration with 5 mL feed volume for 5.3 mg/mL load.

As seen in Figs. 3 and 4B, the gradient slope also affects both peak shape and recovery in a pronounced way. For the high load of Fig. 3, increasing the gradient duration from 10 to 20 CV results in a broader peak eluting at somewhat higher salt concentrations, which is the trend normally expected in gradient elution HIC when retention increases monotonically as the salt concentration increases [21,22]. The recovery also increases reaching close to 100% for this condition as seen in Fig. 4B. On the other hand, decreasing the gradient length from 10 to 5 CV results in an eluted peak that is initially very sharp but that ends in a long tail. Correspondingly, the recovery within 5 CV after the end of the gradient decreases to only about 85%. This behavior occurs because of the U-

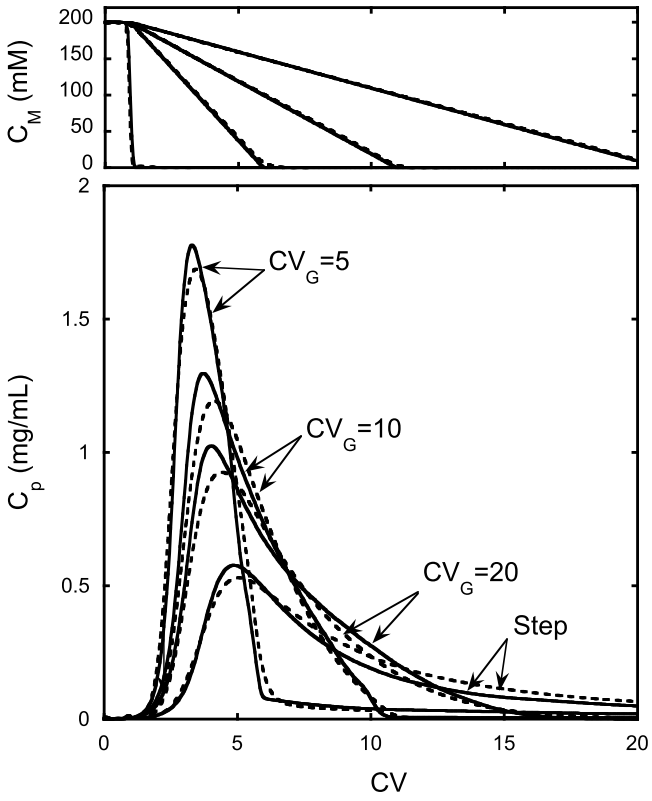

Fig. 3. Comparison of the experimental gradient elution profiles (dashed lines) obtained using different gradient slopes shown by curve labels with model predictions (solid lines) using linear gradient from 0.2 to 0 M ammonium sulfate with 5.3 mg/mL protein load. Experimental loads were realized by injecting 5 mL of feed containing 3.9 mg/mL protein.

shaped retention curve, which allows the low salt concentrations occurring later in the gradient to catch-up with protein molecules still held in the column causing them to rebind to the resin and elute only slowly way after the gradient has ended. Finally, for the step run, elution did not begin until several CVs after the step passed through the column resulting in a highly tailed peak. In this case, recovery even after 25 CV after the step was only about 80%. This behavior is caused again by the U-shaped retention curve. In this case, the abrupt change from 0.2 to 0 M ammonium sulfate causes a large fraction of the protein to be trapped in the region of high retention at low salt causing a long elution tail. As seen in Fig. 4B, lower recoveries are obtained with the same gradient slope for lowest protein load of 0.3 mg/mL (studied in our prior work [9]) compared to the highest load of 5.3 mg/mL. This occurs because, according to the isotherm data in Fig. 1 the U-shaped retention behavior is clearly more pronounced at low protein loads than at higher loads as a result of the interplay of changing both initial slope and isotherm shape as a function of ammonium sulfate concentration.

3.4. Model predictions

The model used in this work to predict the elution behavior is the same as that used previously for the low loading case [9], but incorporates the experimentally measured non-linear isotherms. In this model, the LDF approximation based on a liquid phase concentration driving force is used to describe the protein mass transfer kinetics according to the following equation [2,18,23]:

$$\frac{\partial \bar{q}_p}{\partial t} = \frac{60 D_e}{d_p^2}\left(C_p - C_p^*\right) \tag{4}$$

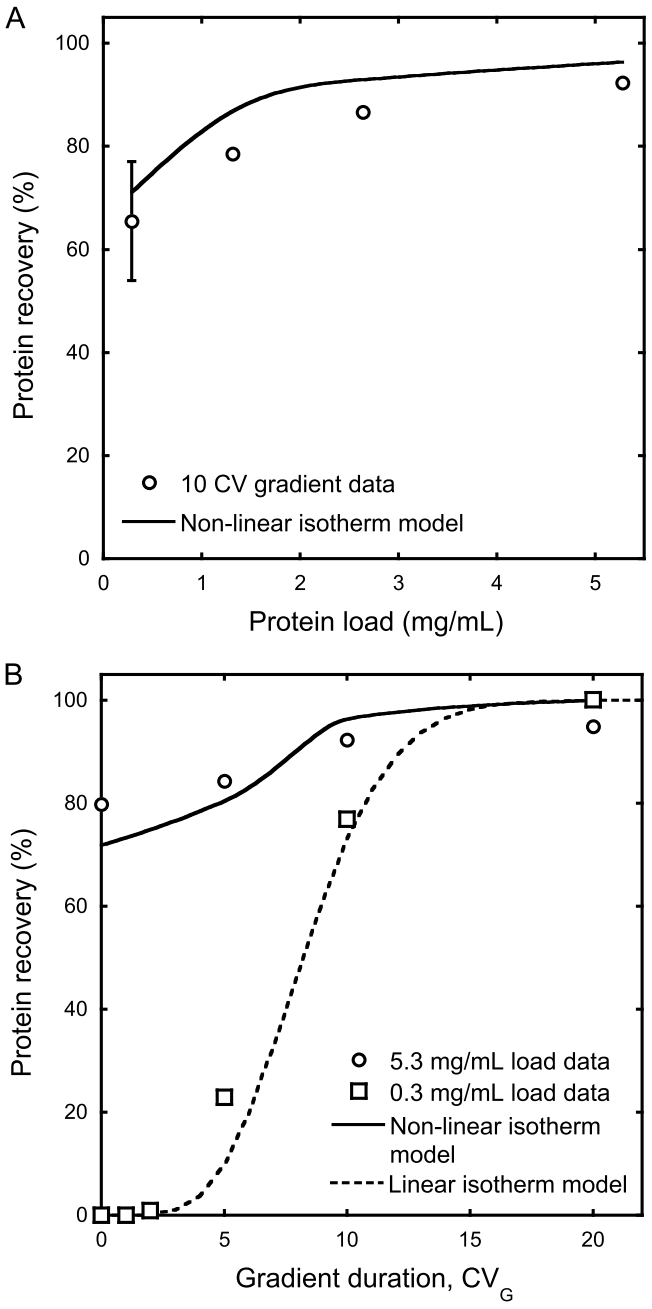

Fig. 4. Protein recoveries obtained within 5 CV after completion of the gradient for the gradient runs and after 25 CV for the step elution case for the runs in Figs. 2 and 3. Panel A shows the results for the runs varying protein loads in Fig. 2 while panel B shows the results for the runs varying gradient slope in Fig. 3. Solid lines are model predictions as described in the text. Squares and dashed lines in panel B are the low loading results at 0.3 mg/mL load from Creasy et al. [9].

where D_e is the protein effective pore diffusivity and C_p^* is the protein solution concentration at equilibrium with $\bar{q}_p$ according to the data in Fig. 1. The value $D_e = 1.0 \times 10^{-7}$ cm^2/s, obtained from our previous study [9], was used in this work. This equation is coupled with the following material balance for the column:

$$\varepsilon \frac{\partial C_p}{\partial t} + (1-\varepsilon)\frac{\partial \bar{q}_p}{\partial t} + u\frac{\partial C_p}{\partial x} = 0 \tag{5}$$

where x is the column axial coordinate and u is the superficial velocity. This equation assumes plug flow and neglects axial dispersion. These assumptions have been validated in our prior work with low protein loads and are expected to be even more appropriate in

this case since a greater proportion of the overall band-broadening effect occurs as a result of the non-linear shape of the adsorption isotherms rather than mass transfer. The coupled Eqs. (4) and (5) were solved numerically by discretizing the axial derivative in Eq. (5) by backwards finite differences over the length of the column, L, and solving the resulting system of ordinary differential equations using MATLAB's multistep, variable order solver routine, *ode15s*. Numerical dispersion caused by the discretization was minimized by using 200 discretization points, which resulted in minimal dispersion of salt profiles and no significant effect on the spreading of protein concentration profiles. All calculations were done in MATLAB R2016a (The Mathworks, Natick, ME, USA) on a Dell Precision T1700, Intel i7 series 3.40 GHz.

The empirical interpolation (EI) method of Creasy et al. [19,20] was used to incorporate the isotherm data in these calculations using the empirical quadratic Langmuir isotherm to correlate the effect of protein concentration at fixed ammonium sulfate concentrations and *pchip* to interpolate between different ammonium concentrations. The latter were generated along the column by solving equations analogous to Eqs. (4) and (5) for ammonium sulfate. The aqueous diffusivity of ammonium sulfate was determined by Wishaw and Stokes [24] to be $(0.83 \pm 0.03)\text{x}10^{-5}$ cm^2/s in the 0–0.2 M concentration range. The effective diffusivity in the particles is expected to be somewhat smaller. However, simulations using different values of D_e for ammonium sulfate in the range 10^{-5} to 10^{-7} cm^2/s gave results for both the gradient and the ensuing protein elution peak that were only minimally dependent on the exact value of D_e (see Fig. S4 in the Supplementary material). As a result, simulations with a high D_e value for ammonium sulfate predicted nearly ideal salt gradients in close agreement with the experimental ones. In order to generate a fast look–up table of isotherm values for column simulations, a grid of 50×50 values for 50^2 combinations of C_M and C_p values were given as inputs to MATLAB's function *griddedInterpolant*. The function uses bilinear interpolation to quickly return $\bar{q}_p$ values for a given input of C_M and C_p. An inverse interpolating function was then used to return corresponding equilibrium protein liquid concentration C_p^* for use in Eq. (4) if the independent variables passed to the *griddedInterpolant* function are C_M and $\bar{q}_p$ values. The same approach has been demonstrated to be effective for the prediction of overloaded elution profiles in ion exchange columns using either salt gradients, pH gradients, or combinations of salt and pH gradients. Since the adsorption isotherm data are used directly without employing a mechanistic model, the approach is useful for cases such as ours where a thermodynamic description of the isotherm is not available.

Elution curves and recoveries predicted by the model are shown in Figs. 2 and 3 and in Fig. 4, respectively. As seen in these figures, both predicted elution profiles and recoveries are in agreement with the data confirming that the observed LGE results are fully consistent with the isotherm behavior. The model does predict somewhat higher recoveries than observed experimentally as a function of protein load but it should be noted that the calculation of recovery from the experimental data is itself potentially affected by significant error because of the tailing peak shapes. Moreover it should be noted that these are true predictions based on the batch isotherm data without any adjustment of model parameters. The predicted trends are nevertheless in substantial agreement with the data suggesting that the model can be used, on one hand, to understand the complex experimental behavior of this system while, on the other, to predict its practical impact.

An important consideration is the effect of the final ammonium sulfate concentration in the gradient on the shape of the eluted peaks and the protein recovery. This effect is illustrated in the Supplementary Material as an application of the model developed in this work. As expected, the model predicts that if the final ammonium sulfate concentration in the gradient is higher than 0.05 M, which corresponds to the minimum in the retention factor curve, or if the gradient is sufficiently shallow that the protein elutes before this concentration is attained in the column and does not get trapped in the column in the down-sloping region of this curve, then the elution peaks have the normal behavior expected for a monotonic retention factor curve. In this case, steeper slopes result in narrower peaks. Elution can still be delayed, though, as the protein is retained significantly even at the end of the gradient and can continue to elute after the column has reached the final ammonium sulfate concentration. Figs. S1–S3 in the Supplementary material illustrate these effects at both low and high protein loads as a function of the gradient slope for 0 and 0.05 M final ammonium sulfate concentrations.

4. Conclusions

The protein load affects the gradient elution chromatographic behavior of a protein exhibiting a U-shaped retention factor curve as a function of ammonium sulfate in HIC in a complex way. Both peak shape and protein recovery are affected. The peaks transition from fronting to tailing and the recovery within the gradient increases as the protein load increases as a result of the non-linear shape of the adsorption isotherm at higher protein loads. The gradient slope at high protein loads also affects peak shape and recovery, with the latter being lowest with the steepest gradient slopes. The effect of the gradient slope is however less pronounced than observed previously at low protein loads as the U-shaped effect of ammonium sulfate on binding is less pronounced at higher protein loads compared to the infinite dilution case. In either case, the nearly quantitative agreement of a dynamic model incorporating the batch isotherm data with the experimental elution profiles confirms that the observed chromatographic behavior indeed results from the complex adsorption equilibrium isotherms. A unique feature of the model developed in this work is that it predicts how protein recovery, as influenced by the U-shaped retention behavior as a function of salt concentration, is affected by protein loading and gradient slope.

A final consideration is given to the underlying biomolecular mechanisms that are responsible for the U-shaped retention factor curves in the dilute limit and for the shifting isotherm shapes observed for overloaded conditions. It is possible that this behavior is associated with the potential existence of hydrophobic domains on the protein surface, especially since the operating pH of 7.2 is not far from the protein pI. However, a definitive conclusion in this regard is not possible without detailed knowledge of molecular details. Other biomolecular reasons, such as the potential presence of charge variants or glycoforms in the antibody sample used, can also be considered. However, it does not appear that molecular microheterogenity could be responsible for the major features of the observed behaviors, such as recovery that decreases with steeper gradients or elution with a reverse ammonium sulfate gradient (i.e. with increasing concentration) that was reported in our previous paper [9].

Acknowledgement

This research was supported by Bristol-Myers Squibb.

Appendix A. Supplementary data

Supplementary material related to this article can be found, in the online version, at doi:https://doi.org/10.1016/j.chroma.2018.10.003.

References

[1] A.A. Shukla, J. Thommes, Recent advances in large-scale production of monoclonal antibodies and related proteins, Trends Biotechnol. 28 (2010) 253–261.
[2] G. Carta, A. Jungbauer, Protein Chromatography – Process Development and Scale-up, Wiley-VCH, 2010.
[3] S.M. Cramer, M.A. Holstein, Downstream bioprocessing: recent advances and future promise, Curr. Opin. Chem. Eng. 1 (2011) 27–37.
[4] W. Melander, Cs. Horvath, Salt effect on hydrophobic interactions in precipitation and chromatography of proteins: an interpretation of the lyotropic series, Arch. Biochem. Biophys. 183 (1977) 200–215.
[5] W.R. Melander, D. Corradini, Cs. Horvath, Salt mediated retention of proteins in hydrophobic-interaction chromatography, J. Chromatogr. 317 (1984) 67–85.
[6] M. Baca, J. De Vosa, G. Bruylants, K. Bartik, X. Liu, K. Cook, S. Eeltink, A comprehensive study to protein retention in hydrophobic interaction chromatography, J. Chromatogr. B 1032 (2016) 182–188.
[7] A.A. Green, Studies in the physical chemistry of the proteins. X. The solubility of hemoglobin in solutions of chlorides and sulfates of varying concentration, J. Biol. Chem. 95 (1932) 47–66.
[8] IUPAC, Compendium of Chemical Terminology, 2nd ed., Blackwell Scientific Publications, Oxford, 1997 (the G̈old Book̈). Compiled by A. D. McNaught and A. Wilkinson.
[9] A. Creasy, J. Lomino, G. Barker, A. Khetan, G. Carta, Gradient elution behavior of proteins in hydrophobic interaction chromatography with U-shaped retention factor curves, J. Chromatogr. A 1547 (2018) 53–61.
[10] GE Healthcare, Instructions 28-9955-33AB, Hydrophobic Interaction media Capto™ Phenyl (High Sub), 2011.
[11] C. Machold, K. Deinhofer, R. Hahn, A. Jungbauer, Hydrophobic interaction chromatography of proteins I. Comparison of selectivity, J. Chromatogr. A 972 (2002) 3–19.
[12] J.M. Mollerup, A review of the thermodynamics of protein association to ligands, protein adsorption, and adsorption isotherms, Chem. Eng. Technol. 31 (2008) 864–874.
[13] F. Xia, D. Nagrath, S.M. Cramer, Modeling of adsorption in hydrophobic interaction chromatography systems using a preferential interaction quadratic isotherm, J. Chromatogr. A 989 (2003) 47–54.
[14] J. Chen, S.M. Cramer, Protein adsorption isotherm behavior in hydrophobic interaction chromatography, J. Chromatogr. A 1165 (2007) 67–77.
[15] Q. Meng, J. Wang, G. Ma, Z. Su, Isotherm type shift of hydrophobic interaction adsorption and its effect on chromatographic behavior, J. Chromatogr. Sci. 51 (2013) 173–180.
[16] G. Wang, T. Hahn, J. Hubbuch, Water on hydrophobic surfaces: mechanistic modeling of hydrophobic interaction chromatography, J. Chromatogr. A 1465 (2016) 71–78.
[17] R. Deitcher, J. Rome, P. Gildea, J. O'Connel, E. Fernandez, A new thermodynamic model describes the effects of ligand density and type, salt concentration and protein species in hydrophobic interaction chromatography, J. Chromatogr. A 1217 (2010) 199–208.
[18] D.M. Ruthven, Principles of Adsorption and Adsorption Processes, Wiley, New York, 1984.
[19] A. Creasy, G. Barker, Y. Yao, G. Carta, Systematic interpolation method predicts protein chromatographic elution from batch isotherm data without a detailed mechanistic isotherm model, Biotechnol. J. 10 (2015) 1400–1411.
[20] A. Creasy, G. Barker, G. Carta, Systematic interpolation method predicts protein chromatographic elution with salt gradients, pH gradients and combined salt/pH gradients, Biotechnol. J. 12 (2017), 1600636.
[21] L.R. Snyder, Gradient elution, in: Cs. Horvath (Ed.), High-Performance Liquid Chromatography–Advances and Perspectives, vol. 1, Academic Press, New York, 1980, pp. 208–314.
[22] S. Yamamoto, M. Nomura, Y. Sano, Resolution of proteins in linear gradient elution ion-exchange and hydrophobic interaction chromatography, J. Chromatogr. 409 (1987) 101–110.
[23] M.D. LeVan, G. Carta, in: D.W. Green (Ed.), Adsorption and Ion Exchange, Section 16, in Perry'S Chemical Engineers' Handbook, 8th ed., McGraw–Hill, New York, 2007.
[24] B.F. Wishaw, R.H. Stokes, The diffusion coefficients and conductances of some concentrated electrolyte solutions at 25°, J. Am. Chem. Soc. 76 (1954) 2065–2071.